Physica E 138 (2022) 115047

Contents lists available at ScienceDirect

Physica E: Low-dimensional Systems and Nanostructures

journal homepage: www.elsevier.com/locate/physe

Influence of irradiation by Swift Heavy Ions (SHI) on electronic magnetotransport in Sb δ-layer in silicon

Alexander K. Fedotov [a], Uladzislaw E. Gumiennik [a,b,*], Vladimir A. Skuratov [c,d,e], Dmitry V. Yurasov [f], Julia A. Fedotova [a], Alexey V. Novikov [f,g], Alexander S. Fedotov [h,i], Pavel Yu. Apel [d,e]

[a] Institute for Nuclear Problems, Belarusian State University, Babrujskaja Str. 11, Minsk, 220006, Belarus
[b] AGH University of Science and Technology, Mickiewicza Av. 30, Kraków, 30-059, Poland
[c] Joint Institute for Nuclear Research, Joliot-Curie Str. 6, Dubna, 141980, Russia
[d] Dubna State University, Universitetskaya Str. 19, Dubna, 141982, Russia
[e] National Research Nuclear University MEPhI, Kashirskoe shosse 31, Moscow, 115409, Russia
[f] Institute for Physics of Microstructures, Russian Academy of Sciences, GSP-150, Nizhny Novgorod, 603950, Russia
[g] Lobachevsky State University of Nizhny Novgorod, Gagarina Av. 23, Nizhny Novgorod, 603022, Russia
[h] Belarusian State University, Niezaliežnasci Av. 4, Minsk, 220030, Belarus
[i] University of Tyumen, Volodarskogo Str. 6, Tyumen, 625003, Russia

ARTICLE INFO

MSC:
00-01
99-00

Keywords:
δ-layer
Swift heavy ions
Irradiation
Magnetoresistance
Weak localization

ABSTRACT

In the present paper we report about the influence of Swift Heavy Ions (SHI) irradiation on the electron transport in a silicon structure containing δ-layer heavy-doped with antimony. Temperature and magnetic field dependencies of the sheet resistance $R_{Sq}(T, B)$ in the temperature range $2 < T < 300$ K and magnetic field induction (B) up to 8 T of the structure before and after the 167 MeV Xe^{+26} ion irradiation with $1 \cdot 10^8$ cm^{-2} – $5 \cdot 10^{10}$ cm^{-2} ion fluences (D) were measured. The observed $R_{Sq}(D, T)$ curves for δ-layer have shown the competition between formation and annealing of defects induced by SHI irradiation due to electron stopping mechanism of ion energy loosing. Besides, at temperatures below 50 K, we observed the transition from exponential dependencies of $R_{Sq}(T)$ to a semi-logarithmic $R_{Sq} \sim -\lg(T)$ ones both before and after the SHI exposure. Such behavior confirms the assumption that the low-temperature carrier transport is carried out mainly by the δ-layer. Moreover, transition from positive (PMR) to negative (NMR) relative magnetoresistance $MR(B)$ was observed when temperature decreasing. The appropriate characteristic times for the carrier scattering process in δ-layer at temperatures below 25 K were estimated from $R_{Sq}(T, B)$ dependencies using the theory of 2D quantum corrections to Drude conductivity due to interference of electrons moving by self-crossing routes inside of δ-layer. Fitting of $R_{Sq}(T, B)$ curves in frameworks of this theory indicates prevailing of phase breaking of electrons' wave function due to their scattering on weakly-localized defect centers induced by SHI irradiation.

1. Introduction

Sharp and nanometer-scale width profiles of dopant distribution in semiconductors (known as δ-layers) are the subject of interest for two main reasons. Firstly, they are interesting for fabrication of nanoscale electronic devices. In particular, δ-doping of silicon (Si) by antimony (Sb) has received much attention in view of possible application in such devices as tunnel diodes [1,2], heterojunction bipolar transistors [3,4] and Schottky diodes with reduced barrier height, which are used in radio imaging systems in the millimeter wavelength range providing detection without bias voltage [5]. The creation of sharp profiles of n–type dopants (Sb, P and As) in Si during molecular beam epitaxy (MBE) growth is challenging due to their pronounced surface segregation [6–9] and so requires some efforts to overcome. Secondly, δ-layers are in metallic side of Mott metal–insulator transition that makes them interesting objects for the study of such fundamental properties of low-temperature carrier transport like hopping and quantum interference contributions into conductivity, spin-resolved effects, etc. [1]. In this sense, δ-layers embedded into the semiconducting matrix become one of the mostly typical 2D electronic systems, where it is possible to obtain the electron sheet concentrations in a rather wide range, up

* Corresponding author at: Institute for Nuclear Problems, Belarusian State University, Babrujskaja Str. 11, Minsk, 220006, Belarus.
E-mail address: uladzislaw.gumiennik@gmail.com (U.E. Gumiennik).

https://doi.org/10.1016/j.physe.2021.115047
Received 24 June 2021; Received in revised form 19 October 2021; Accepted 29 October 2021
Available online 10 December 2021

to the very high values of about ~ 10^{14} – 10^{15} cm^{-2} [5]. But, the electron mobility in δ-layers is usually very low, in comparison with hetero-junctions, due to the pronounced contribution of the elastic and inelastic scattering of carriers on the impurity atoms and defects. Just this peculiarity of δ-layers creates the appropriate conditions for the observation of 2D interference quantum corrections (QCs) to Drude conductivity, due to weak localization effects at the presence of self-crossing carriers' trajectories [10–12]. These phenomena, as is known, allow to extract the information about the changes in Thouless lengths and characteristic times of pulse relaxation because of phase breaking of electron wave functions due to external influences (temperature, magnetic field, defects, etc.).

On the other side, defects are ubiquitous in semiconducting samples and play an important – if not imperative – role in properties of both 3D and 2D materials and, as mentioned above, performance of any devices on their base (see, for example, [12] and References therein). Thus, many independent studies have targeted the artificial introduction of defects into 2D materials using irradiation by ions with different energies (low-, medium-, as well as swift heavy ions (SHI), in particular), see for example, [13–15] and References therein. When SHI enters inside the semiconductor, it loses its energy through electronic and nuclear energy loss mechanisms. But in near-surface δ-layers, the electronic energy loss is dominated whereas the nuclear energy loss becomes dominant only at the end of the projected range of ion, i.e. in the depth of the substrate [15]. Thus, it is natural to expect after SHI exposure noticeable changes in electronic properties inside the near-surface part of Si-based nanostructures due to effects of lattice ionization, intermixing as well as partial annealing of the induced defects.

In this connection, it would be beneficial to develop general defect engineering strategies for 2D Si-based nanostructures relying on a thorough understanding of defects formation mechanisms under SHI irradiation, which may significantly vary from the ones relevant for 3D materials [16].

So, the goal of this paper is to study the changes in 2D carrier transport characteristics in silicon with 2D δ-layer of Sb caused by defects induced by SHI exposure with low fluences.

2. Experimental procedures

The samples with δ-layer of Sb were fabricated on 12 Ω cm Si (100) substrates and are schematically shown in Fig. 1a. The growth was performed by solid-source MBE on the Riber SIVA-21 machine. Si was deposited using E-Beam evaporator, while Sb was deposited from the standard effusion cell. The growth temperature was controlled by specially calibrated thermocouple and the IR pyrometer IMPAC IS 12 [17]. Si growth rate was controlled using quadrupole mass-spectrometer and quartz thickness sensor.

After standard cleaning of Si (001) substrate, Si buffer 100 nm thick layer was deposited at 550 °C. Subsequently the antimony δ-layer was fabricated using the selective doping technique described in [17]. In particular, the temperature was dropped down to 350 °C, and a certain amount of Sb (~0.3 ML) was deposited and then capped by thin Si layer at such a low temperature. This allowed to obtain a sharp rise of Sb concentration in δ-layer. In order to obtain a sharp drop of Sb bulk concentration (and thus to complete the δ-layer formation) the growth was interrupted and temperature was raised up to 535 °C followed by growth of Si capping layer at this temperature. Due to the very high value of segregation ratio at 535 °C [18], the Sb incorporation into Si layer grown at 535 °C was negligible that allowed to obtain the desired sharp decrease of Sb bulk concentration and so to form the δ-doped layer with abrupt boundaries. Indeed, SIMS measurements have revealed that the top Si layer (of about 70–75 nm thick) had rather low concentration of Sb of the order of ($5 \cdot 10^{15} – 1 \cdot 10^{16}$) cm^{-3}. Therefore, as is seen from Fig. 1a, the structure $Si_{2epi}/\delta\text{-}layer/Si_{1\ epi}/Si_{sub}$ to be measured contained multiple layers: two lightly-doped epitaxial Si_{epi} layers 4 and 6, heavy-doped δ-layer 5 and Si substrate 3.

After growing of epitaxial structures (shown in Fig. 1a), 8 contact pads were prepared by photolithography method (Fig. 1b). Two current contacts (numerated 1–2) and four potential contacts (numerated 7–10) were mounted on a special measuring platform using copper microwires ultrasonically soldered by indium to the contact pads. This made it possible to measure electrical sheet resistance R_{Sq} using the four potential probe method. To check the ohmic behavior of all contacts, we also measured the current–voltage (I-V) characteristics between 1–2 contacts. I–V curves have shown strictly linear shape in the whole temperature range (Fig. 1c) that confirms their ohmic behavior.

To characterize the structural properties of the as-grown samples with δ-doped layers, we have used SIMS, capacitance–voltage (C–V) and TEM measurements. Distribution of Sb atoms obtained by SIMS for one of the typical structures is shown in Fig. 2a in which the heavily doped δ-Sb layer is clearly seen (Sb concentration of the order of $1 \cdot 10^{19}$ cm^{-3}) along with nominally undoped top and bottom Si layers (Sb concentration of the order of $1 \cdot 10^{16}$ cm^{-3}). However, we believe that the observed Sb concentration in undoped layers is largely overestimated due to the SIMS sensitivity limitations (nearly constant Sb concentration in undoped layers is the "parasitic background" and should not be considered as a reliable value) and so the real Sb concentration in undoped Si layers is much smaller. The results of C–V measurements in Fig. 2b confirm the enrichment of the heavily-doped δ-layer with electrons and their low concentration in top and bottom Si layers. Taking into account that fluences of SHI irradiation were low (by reasons mentioned above).

The cross section TEM image of the initial (before irradiation) structure did not observed any differences from surrounding Si epi-layers and substrate that shows high crystalline quality of δ-layer. Taking into account that fluences of SHI irradiation were low (for the reasons mentioned below), we can hardly expect any significant changes in the structure of the δ-layer after irradiation. We only note that the main defects will appear in this case only at the end of the mean projective range of ions, i.e. in the substrate.

Samples were irradiated by 167 MeV Xe^{+26} ions with fluences $D = 1 \cdot 10^{8}$ cm^{-2} – $5 \cdot 10^{10}$ cm^{-2} at the Flerov Laboratory of Nuclear Reactions in Joint Institute for Nuclear Research (Dubna, Russia) using the IC-100 cyclotron. The type of ions was chosen so that it did not give additional doping. The values of the irradiation fluences were chosen weak enough so that they would not lead to intermixing, and also did not introduce significant damages into the δ-layer, which would lead it to an amorphous state or to Anderson's localization [15,16,19,20].

Temperature and magnetic field dependencies of I–V and $R_{Sq}(T, B)$ were measured in the temperature range of $2 < T < 300$ K and magnetic fields up to 8 T both before and after the SHI irradiation. These measurements were performed using the High Field Measurement System (HFMS) supplied with a closed cycle refrigerator (Cryogenic Ltd., London). The sample to be measured was mounted in a special contact platform which was linked to measuring system containing temperature and magnetic field sensors, as well as special shields with heaters around sample to be measured. The measuring platform with the mounted sample was inserted into the channel of superconducting solenoid in the HFMS and connected to an automated electronic measuring system. The current through the sample was controlled by the Sub-Femtoamp Remote SourceMeter Keithley 6430, which made it possible to detect the I–V curves and electrical resistance of the sample in the range of 100 μΩ – 10 GΩ with accuracy not worse than 0.1%. The temperature of the samples was controlled by LakeShore $GaAs$ thermodiodes calibrated with an accuracy of 0.0005 K and having a reproducibility of 0.001 K. To stabilize and measure the temperature with an accuracy of 0.005 K, during scanning of B or sweeping-out of I–V characteristics, we used the LakeShore 331 controller. The error of the sheet resistance R_{Sq} detecting was about 1%, which was mainly due to the inaccuracy in the samples geometric dimensions measurement and also measurements of the potential electrical contacts width and distances between them.

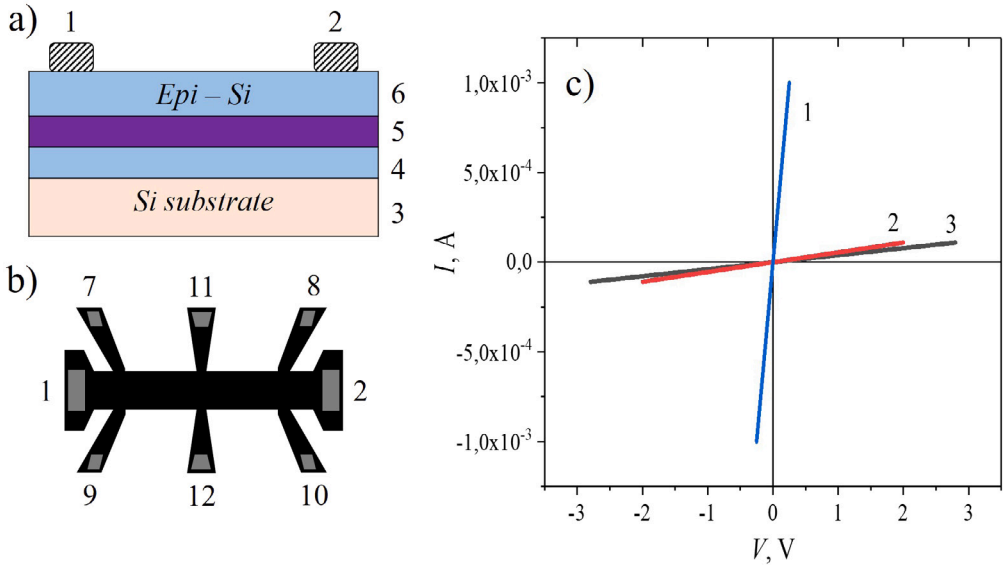

Fig. 1. A schematic cross-view image of the studied sample with δ-layer of Sb in Silicon (a), its top-view image with the electric contact pads (b) as well is its $I-V$ characteristics (c). Designations in (a): 1, 2 – metallic electric contacts, 3 – Si_{sub} - substrate, 4 – buffer Si layer (Si_{1epi}), 5 – δ-doped layer, 6 – top Si layer (Si_{2epi}). In (b): 7, 8 and 9, 10 – potential electric contacts; 11, 12 – Hall contacts. Designations in (c): 1 – 300 K, 2 – 50 K, 3 – 2 K.

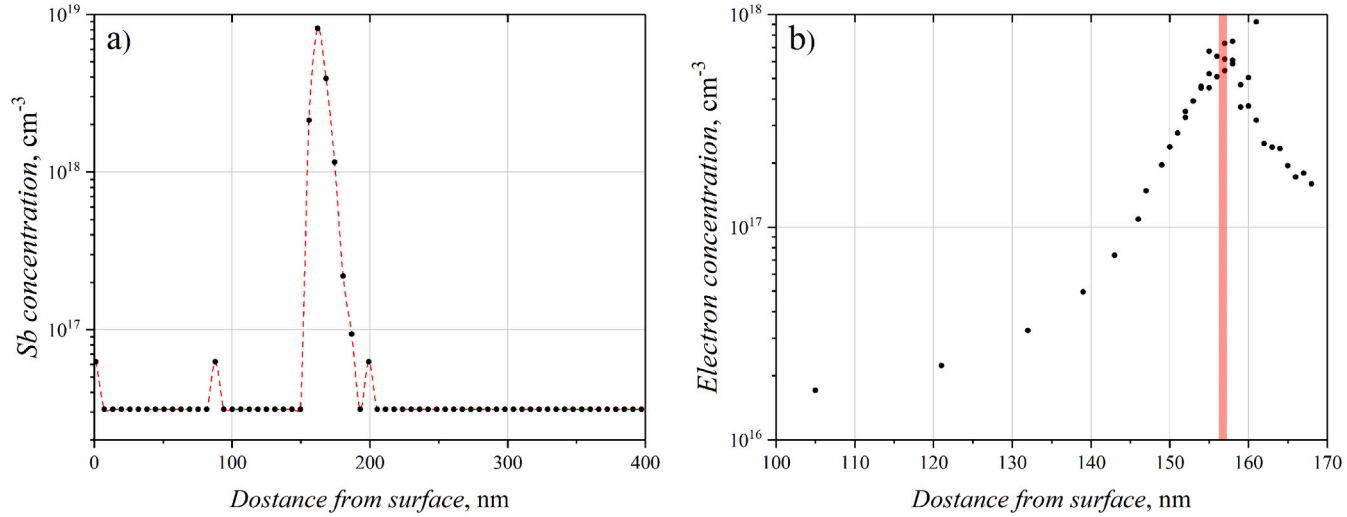

Fig. 2. (a) – Sb atomic distribution obtained by SIMS; (b) – electron distribution obtained by C–V measurements.

3. Results

Our previous studies [21,22] have shown that the current distribution between layers in the studied structure $Si_{2epi}/\delta\text{-}layer/Si_{1\ epi}/Si_{sub}$ was rather complicated in the studied range of temperatures. This is reflected by two very important characteristics of $R_{Sq}(T, D)$ dependencies presented in Fig. 3. Firstly, we note that curve 2 for $D = 1 \cdot 10^8$ ion/cm^2 lies lower than the curve 1 for pristine structure (i.e. at $D = 0$). Second peculiarity consists in the specific shape of temperature dependencies of sheet resistance $R_{Sq}(T)$ in double logarithmic scale (in-set in Fig. 3). As is seen, at $T > 200$ K current is flowing mainly through 450 μm thick Si substrate that was confirmed in [22] by linearization of $R_{Sq}(T)$ curves in Arrhenius scale at $200 < T < 300$ K with the slopes close to the half-width of Si band gap. At the same time, below 25 K, carrier transport in substrate and two epilayers are freezed-out, so that all the current mainly goes through the thin heavy-doped δ-layer.

The described changing in temperature dependencies of $R_{Sq}(T)$ in Fig. 3 with the SHI fluence growth becomes apparent difference in accumulation of defects (due to SHI irradiation) in different components of the studied $Si_{2epi}/\delta\text{-}layer/Si_{1\ epi}/Si_{sub}$ multi-layered structure. This is strongly confirmed by Fig. 4, where $R_{Sq}(D)$ dependencies, presented for three different temperature ranges of measurements, evidently show strong redistribution of current between layers in $Si_{2epi}/\delta\text{-}layer/Si_{1\ epi}/Si_{sub}$ structure with temperature change. As was mentioned above in accordance with the scheme in Fig. 1, curve 3 in Fig. 4, measured at room temperature, corresponds to the case when the $R_{Sq}(T)$ dependence is determined mainly by the current flowing only through the 450 μm thick Si substrate (due to small thickness of Si epi-layers and δ-layer). At the same time, curve 1, corresponding to the temperature of 10 K, refers to the case, when $R_{Sq}(T)$ behavior is mainly supplied by current flowing mainly through thin heavy-doped δ-layer having very low value of sheet resistance. Situation with curve 2 measured at 100 K is intermediate because the $R_{Sq}(T)$ is connected with all layers in the studied structure $Si_{2epi}/\delta\text{-}layer/Si_{1\ epi}/Si_{sub}$. Monotonous shape of curve 3 in Fig. 4 probably reflects the fact that at high temperatures relative contribution to $R_{Sq}(D)$ is due to accumulation of defects (firstly, latent tracks formation) only in the depth of Si substrate [15].

As follows from Fig. 4, low temperatures curves 1 and 2 evidently show non-monotonous behavior: they go through minimum of

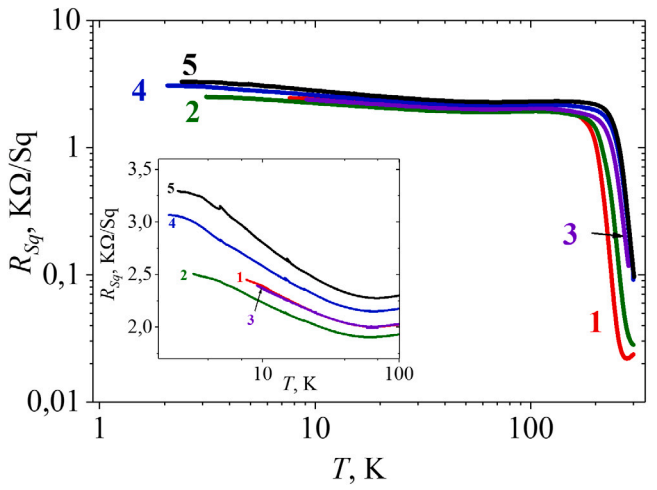

Fig. 3. Temperature dependence of the sheet resistance $R_{Sq}(T)$ in pristine sample (1) and after its SHI irradiation with different fluences D: $1 \cdot 10^8$ (2), $1 \cdot 10^9$ (3), $1 \cdot 10^{10}$ (4) and $5 \cdot 10^{10}$ (5) ion/cm^2. Inset: $R_{Sq}(\lg(T))$ in the structure under study at low temperatures $T < 100$ K.

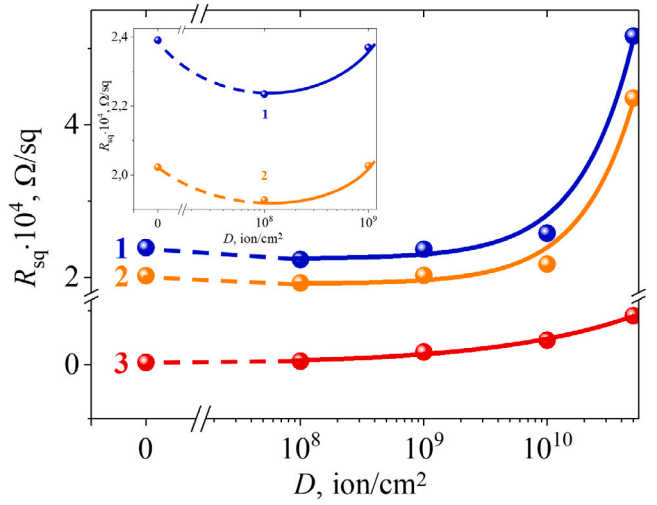

Fig. 4. Dependencies of the sheet resistance $R_{Sq}(D)$ on fluence D in the studied structures for the temperatures 10 K (1), 100 K (2) and 285 K (3). Inset: Low-fluence $R_{Sq}(D)$ curves 1 and 2 in larger scale in the region of minimal $R_{Sq}(D)$ values.

$R_{Sq}(D)$ dependencies at $D = 1 \cdot 10^8$ ion/cm^2. (This correlate with the above-mentioned fact that curve 2 in Fig. 3 after irradiation with $D = 1 \cdot 10^8$ ion/cm^2 goes down as compared with the curve 1 for pristine structure.) We will discuss the possible reasons of such behavior below.

We can also see from Inset in Fig. 3, that below 25 K, when current is flowing only through δ-layer, the $R_{Sq}(T)$ curves for every D value are linearized in semi-log coordinates $R_{Sq} - \lg(T)$. Accordingly [10–12], this indicates that carrier transport in δ-layer can be probably described by the theory of 2D quantum corrections (QCs) into Drude conductance. The tendency of $R_{Sq}(\lg(T))$ dependencies to saturate at temperatures below 5 K can be attributed to the approaching the minimal metallic conductivity σ_{min} due to disordering of δ-layer owing to its closeness to Mott metal–insulator transition [23,24].

Such complicated behavior of carrier transport with temperature in the structure under study impedes its characterization on the basis of the only $R_{Sq}(T)$ dependencies. So, to identify correctly the main contributions into QCs just in the δ-layer before and after SHI irradiation, we have carried out the detailed analysis of relative magnetoresistance $MR(B,T) = [R_{Sq}(B) - R_{Sq}(0)]/R_{Sq}(0)$ measured at temperatures below 25 K in a wide range of magnetic fields. In accordance with [10–12], for 2D weak localization, magnetoresistance of δ-layer at different temperatures can be expressed by the following equation

$$\Delta\rho(B) = -\frac{e^2\rho^2}{\pi h}\left[F\left(\frac{B}{B_\varphi}\right) - F\left(\frac{B}{B_{ee}}\right)\right] \quad (1)$$

$$F(x) = \ln(x) + \psi\left(0.5 + x^{-1}\right) \quad (2)$$

where $\psi(x)$ is the digamma function, the parameter $x = \frac{B}{B_{\varphi,ee}}$. Negative and positive contributions in Eq. (1) characterize phase breaking of electron wave function due to elastic scattering in conditions of low-localization without (first (negative) contribution into $\Delta\rho$ in Eq. (1)) and with accounting the electron–electron interaction (second (positive) contribution into $\Delta\rho$ in Eq. (1)), accordingly. Here,

$$B_{\varphi,ee} = \frac{\hbar}{4D_{diff}e}\tau_{\varphi,ee}^{-1} \quad (3)$$

are characteristic magnetic fields, and τ_i and τ_{ee} – characteristic carriers scattering times for appropriate scattering processes, D_{diff} – diffusion coefficients of carriers. Indices i and ee in Eq. (1)–(3) mean characteristic parameters for quasi-elastic scattering processes without (i) and with (ee) accounting the electron–electron interaction in the interference QCs to Droude conductance.

As is seen from Fig. 5, below 25 K, when current is flowing mainly through δ-layer, we indeed observe the negative (NMR) contribution to the relative magnetoresistance $MR(B,T)$ following from Eq. (1). At the same time, we can see that the values $MR(B,T)$ decrease by modulo followed by the transition to the positive magnetoresistive effect (PMR) when the temperature increases. Taking into account the above-mentioned redistribution of current between the layers of the studied structure with the temperature change, we can attribute the PMR to two contributions: (i) at low magnetic fields (less than 0.5 T) and lower 25 K to QCs taking into account of electron–electron interaction in conditions of low localization and (ii) at magnetic fields $B > 2 - 4$ T and at $T > 50$ K to the acting of Lorentz force on carriers movement in Si substrate and lightly-doped Si epi-layers. Below we discuss the low-magnetic field contributions into NMR and PMR effects using the obtained $MR(B,T)$ dependencies in accordance with Eq. (1).

4. Discussion

Let us firstly discuss the observed changes in carrier transport in the $Si_{2epi}/\delta\text{-}layer/Si_{1\ epi}/Si_{sub}$ structure under impact of SHI irradiation reasoning from the known mechanisms of dissipation of energy introduced to the target by projectile.

As is known from literature [15,19,20], the main processes of slowing down accelerated SHI in matter are the *inelastic collisions* of the incident ions with the target electrons subsystem (the so called, *electronic stopping* mechanism) and the *elastic collisions* with the target nuclei subsystem (*nuclear stopping*). In so doing, if SHI energies are about few hundred MeV, the *electronic stopping* is dominant over the *nuclear stopping* mechanism, especially at the surface of the irradiated structure. In addition, for heavy ions with such energies, nanostructured defects (such as amorphous nanometric latent tracks in the Si substrate depth as well as hillocks at the structure surface [15]) will be produced in the target due to the single-ion impact. Since the transferred energy onto the target structure is very high, we have used very low ion fluences for such artificial modification purpose (not more than 10^{11} ion/cm^2).

Inasmuch as during SHI exposure the energy is mainly transferred to the electronic sub-system near the surface of Si-based structure, it induces different secondary processes of excitations, which result in specific modifications of $epi - Si$ and δ-layers at the top of $Si_{2epi}/\delta\text{-}layer/Si_{1\ epi}/Si_{sub}$ structure. Moreover, as was mentioned above, the main process of slowing down SHI in matter occurs by electronic

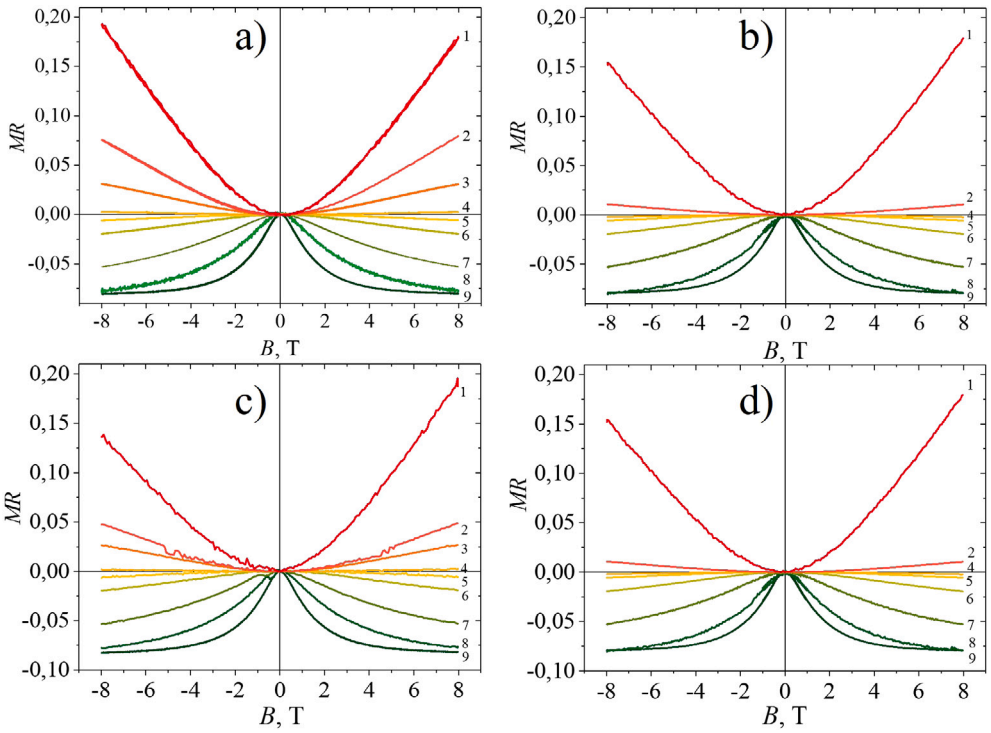

Fig. 5. The examples of $MR(B)$ curves of the studied structure after SHI irradiation with fluences D = 0 (a), $1 \cdot 10^8$ (b), $1 \cdot 10^{10}$ (c) and $5 \cdot 10^{10}$ (d) ion/cm^2 measured at temperatures T: 300 K (1); 200 K (2); 150 K (3); 100 K (4); 50 K (5); 25 K (6); 10 K (7); 5 K (8); 2 K (9).

excitation and ionization processes which provide heating of the lattice subsystem [13]. Thereby, so far as the typical electron stopping of swift heavy ions in most solids is on the order of a few keV per nm, the temperature of the heated lattice can exceed a threshold temperature of defects annealing. Therefore, the decrease of low temperature sheet resistance for $D = 1 \cdot 10^8$ ion/cm^2 (compare $R_{Sq}(T)$ curves 1 and 2 in Fig. 3) can be attributed to the annealing of δ-layer during the second dose of SHI irradiation. This shift to the lower R_{Sq} values gives minimum on $R_{Sq}(D)$ curves 1 and 2 in Fig. 4 at the initial stage of SHI irradiation of the studied structure $Si_{2epi}/\delta\text{-}layer/Si_{1\ epi}/Si_{sub}$. With a further increase of fluence we observe the growth of $R_{Sq}(D)$ (see, curves 1 and 2 in Fig. 4) at $D > 1 \cdot 10^9$ due to probably strong disordering or even amorphization of the epitaxial Si layers and the δ-layer. Note, that monotonous growth of $R_{Sq}(D)$ at room temperature (curves 3 in Fig. 4) probably reflects the accumulation of defects in the depth of Si substrate due to domination of the *nuclear stopping* mechanism at the bottom of latent tracks.

Let us secondly analyze the modification of temperature and magnetic field dependencies of carrier transport properties in δ-layer under impact of SHI irradiation of the $Si_{2epi}/\delta\text{-}layer/Si_{1\ epi}/Si_{sub}$ structure. We shall connect the changes in $MR(T, B)$ behavior with the influence of damages accumulation on mechanisms of electron scattering.

Below, we present the analysis of $MR(T, B)$ and $R_{Sq}(T)$ dependencies using their fitting on the base of the above-mentioned theory of 2D interference quantum corrections to Drude conductivity [10–12]. Fitting of $R_{Sq}(T)$ dependencies was carried out using the relation

$$\left(\frac{\hbar}{\tau_\varphi}\right) = kT \cdot G_0 \cdot R_{Sq} \cdot Ln\left(\frac{1}{\pi G_0 R_{Sq}}\right) \quad (4)$$

taken from paper [10], which is used in the QCs theory when describing phase breaking under conditions of weak localization without taking into account the electron–electron interaction. Here, the phase breaking time τ_φ, according to [25], is described by a power-law temperature dependence of the type

$$\tau_\varphi(T) \sim T^{-p} \quad (5)$$

where the exponent p depends on the carrier scattering mechanism and varies from 1 to 2. The quantum of resistance G_0 in formula (4) is determined by the relation

$$G_0 = \frac{e^2}{2\pi^2\hbar} = 1.23 \cdot 10^{-5}\Omega^{-1} \quad (6)$$

where e is charge of electron and $\hbar$ – normalized Planck constant.

Fitting of $MR(B)$ curves by Eq. (1) was carried out with the only two adjustable parameters B_i and B_{ee} in the temperature range of 2–25 K and at magnetic fields lower than 1 T where NMR was prevailed. The algorithm for the estimation of diffusion coefficients D_{diff} for drifting electrons in (3), based on the experimental values of conductivity, uses the approach of the work [26] and was described in our paper [27].

The results of fitting procedures by Eqs. (1)–(6) are presented in Table 1 and in Fig. 6. Upper indices B and T in the values of τ_φ and p in Table 1 correspond to their values estimated from fitting by Eqs. (1) and (4), respectively. Parameter p was estimated by slopes of linear approximation of $\tau_\varphi(T)$ dependencies in double logarithmic scale in accordance with Eq. (5).

Note the main features of data presented in Table 1 and Fig. 6. We can see that the $\tau_\varphi^B(T)$ and $\tau_\varphi^T(T)$ dependencies correlate between each other, although always $\tau_\varphi^B(T)$ is slightly smaller than $\tau_\varphi^T(T)$. Note also that both dependencies give values $0.95 \le p \le 1.11$ that is close to theoretical value $p \approx 1$ for quantum corrections theory [10–12,25]. We should mention as well that in our case $\tau_{ee} \ll \tau_\varphi$, i.e. taking into account of electron–electron scattering renders weak influence on carrier transport as compared with phase breaking of electron wave functions due to scattering by weakly-localized defect centers in δ-layer induced by SHI.

5. Conclusion

Electron transport in $Si_{2epi}/\delta\text{-}layer/Si_{1\ epi}/Si_{sub}$ structure with Sb δ-layer grown by MBE was studied in detail at temperatures $2 < T < 300$ K and in magnetic fields with induction B up to 8 T before and after SHI irradiation by 167 MeV Xe^{+26} ions with ion fluences $1 \cdot 10^8$ ion/cm^2 ≤

Table 1
Characteristic parameters of quantum corrections to the sheet conductivity of the δ-layer after exposures by different SHI fluences estimated for $T = 10$ K.

Number	*Fluences*, ion/cm^2	D_{diff}, 10^3 m^2/s	$\tau_\varphi^B(T)$, 10^{-12} s	$\tau_\varphi^T(T)$, 10^{-13} s	τ_τ^{ee}, 10^{-14}	p^B	p^T	L_{Th}, nm
1	0	3.76	3.48	7.24	1.15±0.07	1.11	1.03	10.25
2	$1 \cdot 10^8$	4.03	3.69	7.13	1.61±0.12	0.90	1.02	14.08
3	$1 \cdot 10^9$	3.68	–	7.18	–	–	1.02	–
4	$1 \cdot 10^{10}$	3.54	3.95	7.44	1.50±0.15	1.04	1.06	8.53
5	$5 \cdot 10^{10}$	3.21	3.83	7.81	5.19±0.11	0.95	1.09	5.17

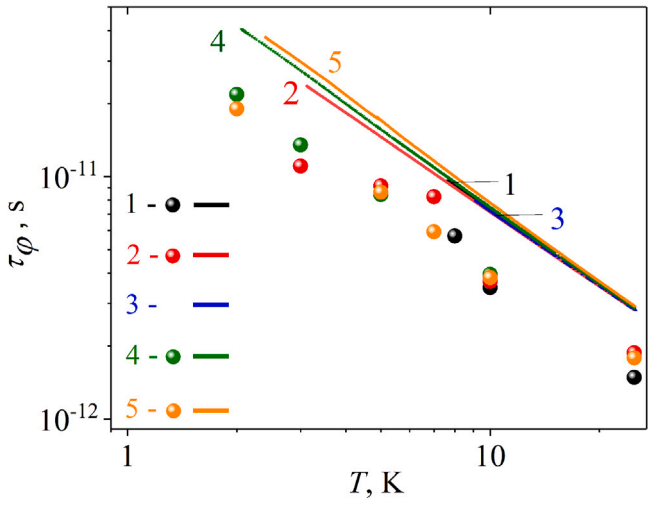

Fig. 6. Temperature dependencies of $\tau_\varphi^B(T)$ (straight lines) and $\tau_\varphi^T(T)$ (dots) for different SHI fluences D, ion/cm^2: 1–0, 2–1 · 10^8, 3–1 · 10^9, 4–1 · 10^{10}, 5–5 · 10^{10}. Lines were estimated from fitting by Eq. (4). Dots positions were determined from fitting by Eq. (1).

$D \leq 5 \cdot 10^{10}$ ion/cm^2. As it was shown for $Si_{2epi}/\delta\text{-}layer/Si_{1\ epi}/Si_{sub}$ structures, when measuring at temperatures below 150 K, the changes in its sheet resistivity $R_{Sq}(D)$ with D growth is determined by electron stopping mechanism and reflects the competition between formation and annealing of defects induced by SHI irradiation at the near-surface region of the structure. At room temperatures the monotonous $R_{Sq}(D)$ dependence was obtained that reflects the influence of nuclear stopping mechanism at the bottom of latent tracks formed in the depth of Si substrate which dominates over electron stopping.

It was shown that the low-temperature carrier transport in δ-layer is described by the theory of two-dimensional quantum corrections to Drude conductivity due to interference of electrons moving by self-crossing routes inside of δ-layer. $R_{Sq}(T, B)$ dependencies for δ-layer show prevailing of phase breaking of interfering electrons due to their scattering on weakly-localized defect centers induced by SHI irradiation.

Declaration of competing interest

The authors declare that they have no known competing financial interests or personal relationships that could have appeared to influence the work reported in this paper.

Acknowledgments

This work was supported financially by the State Program of Scientific Research of Belarus (Minsk, Republic of Belarus) "Material Science, new materials and technologies (Sub-Program "Nanostructured materials, nanotechnologies" (project № 2.13.1). We are also thankful to the Joint Institute for Nuclear Research (Dubna, Russian Federation) for the financial support in the framework of the contract № 08626319/182161170–74 and project № 04-5-1076-2009/2016. The authors are also grateful to Ph.D. I.A. Svito for low-temperature measurements of the electrical properties of samples.

References

[1] Y. Imry, Nanostructures and Mesoscopic Systems, Academic, New York, 1992.
[2] K.D. Hobart, P.E. Thompson, S.L. Rommel, T.E. Dillon, P.R. Berger, D.S. Simons, P.H. Chi, "p-on-n" Si interband tunnel diode grown by molecular beam epitaxy, J. Vac. Sci. Technol. B 19 (1) (2001) 290, http://dx.doi.org/10.1116/1.1339011.
[3] A. Schüppen, H. Dietrich, High speed SiGe heterobipolar transistors, J. Cryst. Growth 157 (1–4) (1995) 207–214, http://dx.doi.org/10.1016/0022-0248(95)00387-8.
[4] A. Gruhle, H. Kibbel, U. König, U. Erben, E. Kasper, MBE-grown Si/SiGe HBT's with high β , f_T, and f_{max}, IEEE Electron Device Lett. 13 (4) (1992) 206–208, http://dx.doi.org/10.1109/55.145022.
[5] A.V. Murel, A.V. Novikov, V.I. Shashkin, D.V. Yurasov, Barrier-height modification in Schottky silicon diodes with highly doped 3D and 2D layers, Semiconductors 46 (11) (2012) 1358–1361, http://dx.doi.org/10.1134/s1063782612110140.
[6] V.B. Krasovitsky, Y.F. Komnik, M. Myronov, T.E. Whall, Quantum interference effects in delta layers of boron in silicon, Low Temp. Phys. 26 (8) (2000) 598–602, http://dx.doi.org/10.1063/1.1289131.
[7] H. Jorke, Surface segregation of Sb on Si(100) during molecular beam epitaxy growth, Surf. Sci. 193 (3) (1988) 569–578, http://dx.doi.org/10.1016/0039-6028(88)90454-2.
[8] H.-J. Gossmann, E.F. Schubert, Delta doping in silicon, Crit. Rev. Solid State Mater. Sci. 18 (1) (1993) 1–67, http://dx.doi.org/10.1080/10408439308243415.
[9] C.B. Arnold, M.J. Aziz, Unified kinetic model of dopant segregation during vapor-phase growth, Phys. Rev. B 72 (19) (2005) http://dx.doi.org/10.1103/physrevb.72.195419.
[10] B.L. Altshuler, A. Aronov, Chapter 1 - electron–electron interaction in disordered conductors, Mod. Probl. Condens. Matter Sci. Elsevier 10 (1985) 153, http://dx.doi.org/10.1016/B978-0-444-86916-6.50007-7.
[11] P.A. Lee, T.V. Ramakrishnan, Disordered electronic systems, Rev. Modern Phys. 57 (2) (1985) 287–337, http://dx.doi.org/10.1103/revmodphys.57.287.
[12] G. Bergmann, Weak localization in thin films, Phys. Rep. 107 (1) (1984) 1–58, http://dx.doi.org/10.1016/0370-1573(84)90103-0.
[13] Z. Li, F. Chen, Ion beam modification of two-dimensional materials: Characterization, properties, and applications, Appl. Phys. Rev. 4 (1) (2017) 011103, http://dx.doi.org/10.1063/1.4977087.
[14] F. Meinerzhagen, L. Breuer, H. Bukowska, M. Bender, D. Severin, M. Herder, H. Lebius, M. Schleberger, A. Wucher, A new setup for the investigation of swift heavy ion induced particle emission and surface modifications, Rev. Sci. Instrum. 87 (1) (2016) 013903, http://dx.doi.org/10.1063/1.4939899.
[15] R. Singh, Studies of modification of transport properties of swift heavy ion irradiated Si and GaAs, (Ph.D. thesis), Jawaharlal Nehru University, 2001.
[16] M. Schleberger, J. Kotakoski, 2D material science: Defect engineering by particle irradiation, Materials 11 (10) (2018) 1885, http://dx.doi.org/10.3390/ma11101885.
[17] F. Aumayr, S. Facsko, A.S. El-Said, C. Trautmann, M. Schleberger, Single ion induced surface nanostructures: a comparison between slow highly charged and swift heavy ions, J. Phys.: Condens. Matter 23 (39) (2011) 393001, http://dx.doi.org/10.1088/0953-8984/23/39/393001.
[18] P.V. Volkov, A.V. Goryunov, A.Y. Luk'yanov, A.D. Tertyshnik, A.V. Novikov, D.V. Yurasov, N.A. Baidakova, N.N. Mikhailov, V.G. Remesnik, V.D. Kuzmin, Optical monitoring of technological parameters during molecular-beam epitaxy, Semiconductors 46 (12) (2012) 1471–1475, http://dx.doi.org/10.1134/s1063782612120214.
[19] H. Xue, Ion irradiation induced damage and dynamic recovery in single crystal silicon carbide and strontium titanate, (Ph.D. thesis), The University of Tennessee, Knoxville, 2015.
[20] M.V. Kumar, S. Verma, V. Shobha, B. Jayashree, D. Kanjilal, R. Ramani, S. Krishnaveni, 100 MeV Si^{7+} ion irradiation induced modifications in electrical characteristics of Si photo detector: An in-situ reliability study, J. Mater. Sci. Res. 3 (3) (2014) http://dx.doi.org/10.5539/jmsr.v3n3p24.

[21] D.V. Yurasov, M.N. Drozdov, A.V. Murel, M.V. Shaleev, N.D. Zakharov, A.V. Novikov, Usage of antimony segregation for selective doping of Si in molecular beam epitaxy, J. Appl. Phys. 109 (11) (2011) 113533, http://dx.doi.org/10.1063/1.3594690.

[22] A.S. Fedotov, V.A. Skuratov, D.V. Yurasov, A.V. Novikov, I.A. Svito, P.Y. Apel, A.K. Fedotov, P.V. Zukowski, V.V. Fedotova, Magnetotransport in Si langle Sb rangle delta-layer after swift heavy ion-induced modification, Acta Phys. Polon. A 132 (2) (2017) 229–232, http://dx.doi.org/10.12693/aphyspola.132.229.

[23] N.F. Mott, Conduction in non-crystalline materials, Phil. Mag. 19 (160) (1969) 835–852, http://dx.doi.org/10.1080/14786436908216338.

[24] N.F. Mott, E.A. Davis, Electronic Processes in Non-Crystalline Materials, Clarendon Press Oxford University Press, Oxford New York, 1979.

[25] V.M. Pudalov, Metallic conduction, apparent metal-insulator transition and related phenomena in two-dimensional electron liquid, in: Proceedings of the International School of Physics “Enrico Fermi”, in: The Electron Liquid Paradigm in Condensed Matter Physics, 157, IOS Press, 2004, pp. 335–356, http://dx.doi.org/10.3254/978-1-61499-013-0-335.

[26] F.V. Tikhonenko, D.W. Horsell, R.V. Gorbachev, A.K. Savchenko, Weak localization in graphene flakes, Phys. Rev. Lett. 100 (5) (2008) http://dx.doi.org/10.1103/physrevlett.100.056802.

[27] A.K. Fedotov, S.L. Prishchepa, A.S. Fedotov, U.E. Gumiennik, I.V. Komissarov, A.O. Konakov, S.A. Vorobyova, A.A. Kharchenko, O.A. Ivashkevich, Effect of cobalt particle deposition on quantum corrections to Drude conductivity in twisted CVD graphene, Mod. Electron. Mater. 5 (4) (2019) 165–173, http://dx.doi.org/10.3897/j.moem.5.4.52068.